JOURNAL OF THE KOREAN ASTRONOMICAL SOCIETY
29: 63 ~ 73, 1996

CHEMICAL EVOLUTION OF THE GALAXY: RADIAL PROPERTIES †

PARK, BYEONG-GON[1,2], KANG, YONG HEE[3] AND LEE, SEE-WOO[4]
[1]Bohyunsan Optical Astronomy Observatory, Korea Astronomy Observatory
Electronic mail : bgpark@seeru.boao.re.kr
[2]Department of Astronomy and Atmospheric Sciences, Kyungpook National University
[3]Department of Earth Science Education, Kyungpook National University
[4]Department of Astronomy, Seoul National University
(Received Mar. 6, 1996 ; Accepted Mar. 18, 1996)

ABSTRACT

The previous study of chemical evolution of the Galaxy is extended to the radial properties of the Galactic disk. The present model includes radial dependency of the time-dependent bimodal IMF, radial flow of material in the disk, and the change of type I supernova explosion rate with radial distance from the disk center as model parameters and observed gas and stellar density distributions and metallicity abundance gradient as observational constraints.

The results of two models in this study explain the observed gas and stellar density distributions well, with the slope of the gas density gradient in the region of 4.5 kpc $< r <$ 12 kpc as $-0.136 dex/kpc$ in model Y_1 and $-0.123 dex/kpc$ in model Y_2, respectively, which fit well the observed gradient of $-0.11 dex/kpc$. The abundance gradient reproduced in model Y_1 is getting flatter with decreasing radius, while that in model Y_2 is getting steeper, which fits better the observed abundance gradient. This result shows the necessity of exponentially increasing type I supernova explosion rate with decreasing radius in order to explain the observed abundance gradient in the disk. The fitness of observed density distribution and star formation rate distribution justifies the reliability of time-dependent bimodal IMF as a compound quantitative chemical evolution model of the Galaxy.

The temporal variations of metallicity gradients for carbon, nitrogen and oxygen are also shown.

Key Words : initial mass function, star formation rate, abundance gradient, chemical evolution

I. INTRODUCTION

The spectroscopic observations of H II regions in our Galaxy and local cluster, and for compesomewhat nsating purpose, of field stars show somewhat large slope of abundance gradient in spiral galaxies (Pagel and Edmunds 1981, Pagel 1985, Garnett and Shields 1987). In the Galaxy, the observed gradient of [Fe/H] and [O/H] is roughly $-0.07 dex/kpc$ with relatively large dispersion(Dufour *et al.* 1980, Shaver *et al.* 1983, Maciel 1991, Belley and Roy 1992). There are some observational results in which the abundance distributions of B stars in young OB associations and distant red giants show no distinguishable metallicity gradient in these stars (Fitzsimmons *et al.* 1990, Neese and Yoss 1988), but it is not certain because of the lack of their data (Gehren *et al.* 1985). Furthermore, the abundance gradient in z-direction also shows lower metallicity farther from the disk which is thought to be resulted from stellar species of different scale heights (Hartkopf and Yoss 1982, Gilmore and Wyse 1985).

The observed radial abundance gradient can be explained using a simple model adapted to each finite equi-centered circle in the disk if the ratio of surface gas density to the overall density decreases with decreasing radial distance from the disk center (Searle and Sargent 1972, Pagel 1981). But the observed density gradient of H I surface density is flat, and even more, the observed increase of the molecular hydrogen in the central region of $r \leq 4$ kpc is not so large to affect the overall density change (Gorden and Burton 1976, Bhat *et al.* 1984, 1985). So in case

† This work was supported by the Basic Science Research Institute Program, Ministry of Education, BSRI-95-5411.

of the simple model, the variation of gas density along the radial distance is not sufficient to explain the observed abundance gradient in the disk (Pagel 1987).

The present model is a radially extended study of the previous halo-disk model which uses the time-dependent bimodal IMF (initial mass function) and power law SFR (star formation rate) as main parameters and observational constraints such as cumulative metallicity distribution with stellar ages, PDMF (present day mass function) of main sequence stars (Lee *et al.* 1991, hereafter referred as paper I). In paper I, we set up a quantitative chemical evolution model which explains many observational properties found in the solar neighborhood such as the G-dwarf problem (van den Bergh 1962, Schmidt 1963, Bond 1970), Wielen dip in the PDMF (Lee and Chun 1986, Scalo 1986), age-metallicity relations (Carlberg *et al.* 1985, Twarog 1980, Nissen *et al.* 1985), age-velocity dispersion relation (Wielen 1977), and various metallicity distributions including carbon, nitrogen, oxygen, and iron (Laird 1985, Carbon *et al.* 1987, Tomkin *et al.* 1986, Tomkin and Lambert 1984).

As an extension of the consecutive studies which have tried to develop a detailed quantitative chemical evolution model of the galaxies (Lee and Ann 1981, Lee and Chun 1986, Lee, Ann and Sung 1989, Park 1991, Lee *et al.* 1991, Kang 1993), this model adopts the $n_2 = 1.4$ model from paper I, with slightly modified IMF which is basically the same form as the original time-dependent bimodal IMF (Lee and Chun 1986). Also in this model, we consider the effect of radial gas flow along the disk and radially increasing SN I (type I supernova) explosion rate in order to describe the observed distributions of the surface density and metallicity.

II. BASIC EQUATIONS

All the basic equations in this paper are the same as those in paper I. Here we refer only those parts of basic equations which include radial dependencies.

The temporal variation of gaseous mass surface density and metal abundance in the disk are written as follows;

$$D\mu_g = -\psi_d(t) + E_{g,d}(t) + f_d(t) - \frac{v_r \mu_g}{r} - \mu_g \frac{\partial v_r}{\partial r} \tag{1}$$

and

$$\mu_g \frac{DZ_d}{Dt} = E_{z,d}(t) - Z_d E_{g,d}(t) + (Z_h - Z_d) f(t). \tag{2}$$

Notational conventions in equations (1) and (2) follow as in paper I. Again, the derivative operator D/Dt is $\partial t + v_r \partial/\partial r$.

For the radial flow velocity v_r, we adopt the central spike model which explains star formation rate, gas density and metallicity distribution in the disk better than the other velocity field models (Lacey and Fall 1985).

In this model, we choose central spike velocity v_1 as $-15 km/s$ at $r_1 = 4$kpc and the velocity in the vicinity of the Sun v_0 as $-0.5 km/s$.

III. MODEL PARAMETERS

As this model is a radial extension of the model in paper I, most model paramaters are the same as in paper I except the IMF in which we added the radial dependency. The resulting IMF used in this paper is now a radial-time dependent bimodal IMF in which the mass spectrum can be written as follows;

$$\phi(\log m, t) = \phi_0(t)\ [w_1 \phi_1(\log m, t) + w_2 \phi_2(\log m, t)] \tag{3}$$

$$\phi_i(\log m, t) = \exp[-B_i(r)(\log m - C_i)^2][\frac{m}{H_i}]^{\gamma_i} \exp[-E_i(\frac{m}{H_i})]^{\beta_i} A(\tau) \tag{4}$$

$$A(\tau) = \frac{1}{1 - G \exp[-(\tau - \tau_0)^2/\delta^2]} \tag{5}$$

where coefficients C_i, H_i, β_i, γ_i, G, τ_0 and δ are constants as in paper I and τ denotes the galactic time in unit of halo formation time scale, with the relation $\tau = 7/15$ Gyr (Lee and Chun 1986). The coefficient B_i, which describes fraction of high mass stars in the IMF varies along the central radius as following;

$$B_i(r) = B_{i,o}\exp[\frac{-(r-r_o)}{r_s}] \tag{6}$$

where $B_{i,o}$ is B_i at the solar neighborhood radius r_o and r_s is scale radius. Note that in the solar neighborhood, $B_i(r)$ becomes the same as $B_{i,o}$. The value of r_o is assumed as 8 kpc in this model.

The normalization constant ϕ_o in equation (3) is defined to give the following relation †;

$$\int_{m_l}^{m_u} \phi(\log m, t)\, m\, dm = 1. \tag{7}$$

where m_l and m_u are assumed as 0.01 $m_\odot$ and 100 $m_\odot$, respectively.

The nature of this IMF is characterized that it will produce more high mass stars near the galactic center. The mass spectrum of new-born stars will have less number of massive stars as the radial distance from galactic center increases.

We calculated two models using the above IMF. Model Y_1 assumes constant SN I explosion rate along the whole disk and model Y_2 assumes exponentially increasing SN I rate toward the Galactic center. The scale length of SN I rate in model Y_2 is assumed as $R_{SN} = 0.8$ kpc. Table 1 summarizes the model parameters used in two models. Note that the exponents of the SFR's are close to unit in both models. As discussed later, the SFR as a power law of gas density can hardly reproduce the observed density gradient if it is nearly linearly proportional to the gas density.

The other assumption in this model is the existence of star birth boundary in the Galactic disk. This assumption is justified by the fact that the outermost radii of the stellar disk in external galaxies are equal to the Holmberg radii and gas layer extends farther than the stellar disk (van der Kruit and Searle 1982, Sancisi 1983). The existence of such boundary in stellar formation is related with the limit of gravitational instability which causes the stellar formation in the outer region of the disk where gas density is lower than some threshold level (Goldreich and Lynden-Bell 1965, Kennicutt 1989). In this model, the star formation cutoff radius is assumed to be 18kpc. The observational evidence for this assumption can be found from $r_{max} = 20$kpc from OB stars in the Galactic anticenter (Chromey 1978), $r_{max} = 16 \sim 20$kpc from H II observation (Fich and Blitz 1984), and $r = 15 \sim 17$kpc for starting radius of gaseous disk warping (Kulkarni *et al.* 1982).

Table 1. Model Parameters

Model	d_1	n_2	α	ϵ	B_1	B_2	C_1	C_2	E_1	E_2	H_1	H_2
Y_1	0.20	1.0	4.0	0.008	0.6	9.0	-3.0	-0.8	33.0	0.01	0.2	0.8
Y_2	0.13	1.1	4.0	0.008	0.6	9.0	-3.0	-0.8	33.0	0.01	0.2	0.8

Model	β_1	β_2	γ_1	γ_2	W_1	W_2	D	t_o	δ	r_s	R_{SN}
Y_1	-3.0	-0.7	-0.7	-0.02	150	1	1.002	0.013	5.0	70	–
Y_2	-3.0	-0.7	-0.7	-0.02	150	1	1.002	0.013	5.0	70	0.8

† The relation between mass spectrum $\phi(m,t)$ and the IMF $\xi(\log m, t)$ is given by $\phi(m,t)dm = \xi(\log m, t)d\log m$, and hence, the normalization of the IMF is given by;

$$\int_{m_l}^{m_u} \xi(\log m, t)\, m d\log m = 1$$

IV. THE NUMERICAL COMPUTATION

To solve the differential equations for the gas, stellar mass and metal abundances in the Galaxy, we set up a numerical model in which we use the IMSL subroutine DVERK based on 4th and 5th order Runge-Kutta method. For equations which involve integration, we use a simple Simpson formula and the quadratic Gaussian integration with 32 quadratic subdivisions (Conte and de Boor 1980).

As the Galaxy evolves rapidly in the early evolutionary phase and relatively slow in the later phase, we divide the age of the Galaxy into 150 intervals in which the time step increases smoothly from the minimum of a few hundreds of thousand years to the maximum of a few giga years. The age of the Galaxy is assumed to be 15 Gyr.

We run this model at the IBM PC 486 compatible computer by iterative way, consuming about 4 hours of the CPU time for one computation.

V. RESULTS AND DISCUSSION

(a) Variation of Physical Quantities along the Galactic Radius

When the IMF is constant upon time and space, the most important factors which affect the metallicity gradient are SFR and the ratio between infall rate from halo and surface gas density (Tinsley 1980, Matteucci and François 1989). The former accelerates metallicity enrichment and the latter lowers the metal abundance by metal poor gas from halo.

In such model, the mean ratio between SFR and infall rate should be assumed to decrease along the galactic radius to explain observed metallicity gradient of the Galactic disk. As the SFR following Schmidt's simple model(Schmidt 1959) depends highly on the distribution of gas, if the exponent of the SFR is high ($n_2 > 2$), metallicity gradient could be generated by assuming the infall rate distribution appropriately to give proper gas density gradient along the disk. But in this case the exponent of the SFR is subject to high observational constraints such as gas density and some major chemical abundances observed in the solar neighborhood (Lacey and Fall 1985, Matteucci and François 1989).

In our models, as the SFR is nearly linearly proportional to the gas density and the infall rate from halo is also proportional to the SFR, it is not expectable to explain the metallicity gradient in the disk by gas density gradient generated by the infall and radial flow, in spite of the use of radially dependent IMF. So we introduced the assumption that the star formation is forbidden in the region outer than some distance from the Galactic center.

The radial distribution of gas and stars are dependent of the infall rate from the halo as well as the SFR, and they also depend indirectly on the radial flow velocity along the disk and the IMF which is involved with the ejected matter from evolving stars. So the observed radial gradient of surface gas density is a strong observational constraint especially for the proper exponents of SFR's expressed in power of gas density, and also it constrains the upper limit of the radial flow velocity in common with the observed distribution of the SFR.

(b) The Distribution of Gas and Stars

In the halo-disk model, the gas density distribution along the disk basically depends on the different amount of infall gas from the halo at different radial circumference of the disk. In this model, the halo evolution does not consider the central radius. Instead, the infall gas from the halo is assumed to have an exponential distribution with a scale length of 4 kpc.

Fig. 1 shows the variation of gas density along the disk radius with time. In Fig. 1a, the sudden decrease of gas matter within 4 kpc occurs because the consumption rate is getting higher by the increasing radial flow in this region. In the outer region of the disk, the density gradient is getting flatter with time. This is caused by the flow of high density gas matter due to the cutoff of star formation at $r > 18$kpc. The increase of gas density in $r > 4$kpc until $t \leq 0.7$Gyr can be explained by ejected matter from massive stars born in the early phase of disk evolution by the time-dependent bimodal IMF. The distribution of gas density in this model fits well the observational evidence of the sudden decrease within 4 kpc from the H I observation of Burton and Gordon (1978) and molecular hydrogen distribution from CO observations by Cohen *et al.* (1984), and also fits well the observed exponential distribution with a scale length of 4 kpc outer than solar radius by Kulkarni *et al.* (1982), Henderson *et al.* (1982). The slope of the gas density gradient in the region of 4.5 kpc $< r <$ 12 kpc is $-0.136 dex/kpc$ in model Y_1 and $-0.123 dex/kpc$

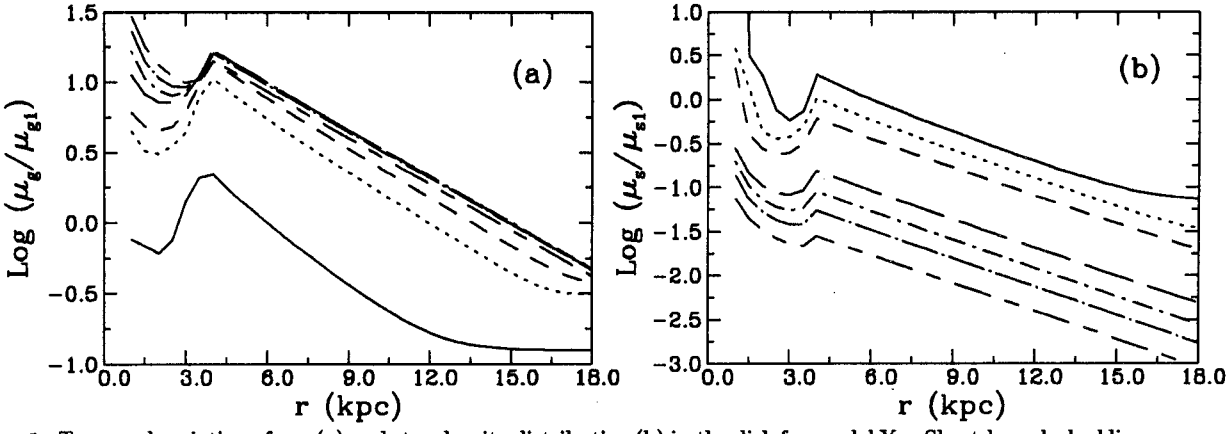

Fig. 1. Temporal variation of gas (a) and star density distribution (b) in the disk for model Y_1. Short-long dashed line represents at t = 0.3Gyr, dotted-long dashed line at t = 0.5Gyr, dotted-short dashed line at t = 0.7Gyr, long dashed line at t = 1Gyr, short dashed line at t = 3Gyr, dotted line at t = 5Gyr and the solid line at t = 15Gyr, respectively.

in model Y_2, and these values are comparable to the mean observed slope of $-0.11 dex/kpc$ presented by Lacey and Fall (1985).

Fig. 1b shows how the the stellar mass density distribution changes along the radial distance. Again the sudden decrease within 4 kpc is related with the radial velocity field effect. The stellar mass density distribution depends on the star formation rate rather than infall from halo and the density decreases with increasing mass ejection rate from dying stars. The monotonous increase of stellar mass density in the region $r > 4$ kpc at $t \leq 0.7$ Gyr in spite of the relatively fast increase of the gas density in this region results from this effect.

(c) The Star Formation Rate

In order to fit the observed radial distribution of the SFR, the SFR following a power law of the gas density should be nearly linearly proportional to the gas density, having the exponent close to unit value. In other evolution models related to fit the observed variation of the SFR with time in the vicinity of the Sun, such a linear relation is recommended (Miller and Scalo 1979, Kennicutt 1983).

Fig. 2a shows the SFR distribution in this model overlapped to the observed radial distribution. Y axis value has been adjusted for comparision with the observation. The SFR distribution in our two models fit quite well the observation. Especially in model Y_2, the exponentially increasing SN I explosion rate with decreasing radius does not show a significant difference from the result obtained by model Y_1 in which a constant rate of SN I explosion is assumed. This is due to the absolute scarceness of SN I in the disk. The shape of the SFR distribution in the disk becomes flatter with time, like the gas density distribution, as shown in Fig. 2b. This phenomenon can be explained in the same way as in the case of the gas density because the SFR is proportional to the gas density.

(d) Abundance Gradient in the Disk

The metallicity distribution in the disk is related with a number of physical processes such as metal ejection from evolving stars, nucleosynthetic process in the stellar interior, SFR and IMF. In Fig. 3a, the computed metallicity distribution is compared with the observed distribution from Lacey and Fall(1985). The two models Y_1 and Y_2 fit well the observed distribution in the region outer than the solar radius (r > 8 kpc). The increasing metallicity gradient with radius is thought to be related with the cutoff in the SFR and the inward supply of unprocessed matter by radial gas flow. Such effect is clear when we consider the change of the metallicity gradient with evolution time as seen in Fig. 3b and Fig. 3c, i.e., the metallicity gradient extends into the Galactic center with time.

Although there are some observation which says that the abundance gradient in the inner region of the disk is flat and independent of the stellar age (Janes 1979, Panagia and Tosi 1981), there is not seen a definite trend of flattening of abundance gradient inward. The flattening of abundance gradient inward the disk center seen in model Y_1 in Fig. 3a is a general phenomenon in evolution models with the infall from the halo (Tosi 1982), which is caused by the dilution of gas by metal-poor infall gas from the halo in this model. In the model Y_2, we introduced the

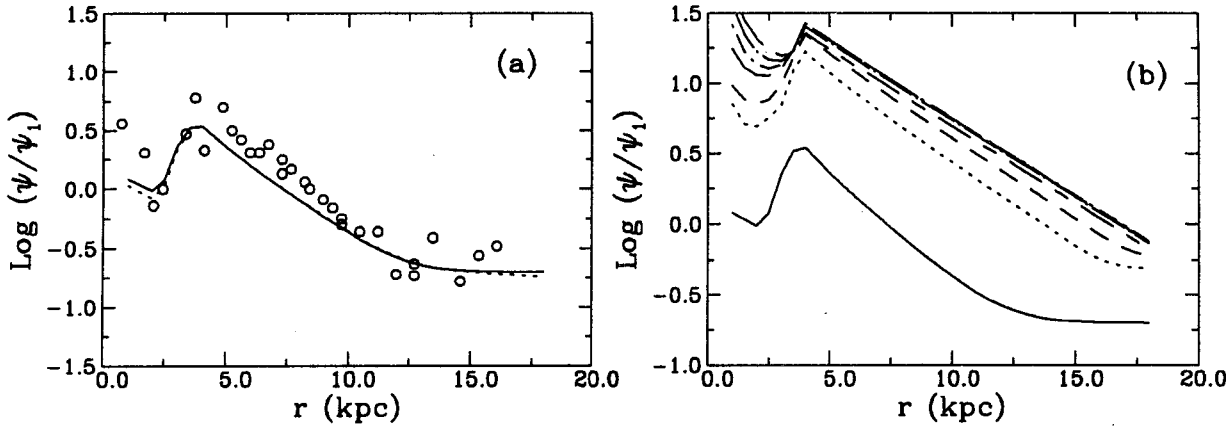

Fig. 2. (a) The radial variation SFR distribution in the disk. Solid line represents for model Y_1 and dotted line represents model Y_2. Observed data are from Lacey and Fall(1985). (b) Temporal variation of the SFR distribution for model Y_1. Line legends are the same as in Fig. 1.

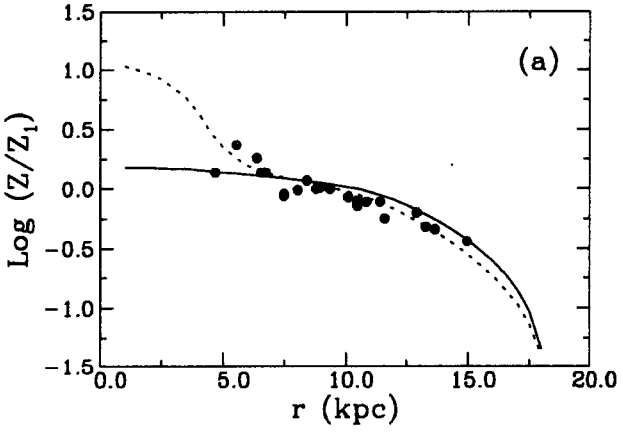

Fig. 3.(a) The radial variation of metal abundance in the disk. Solid line represents model Y_1 and dotted line represents model Y_2. Observed data are from Lacey and Fall(1985).

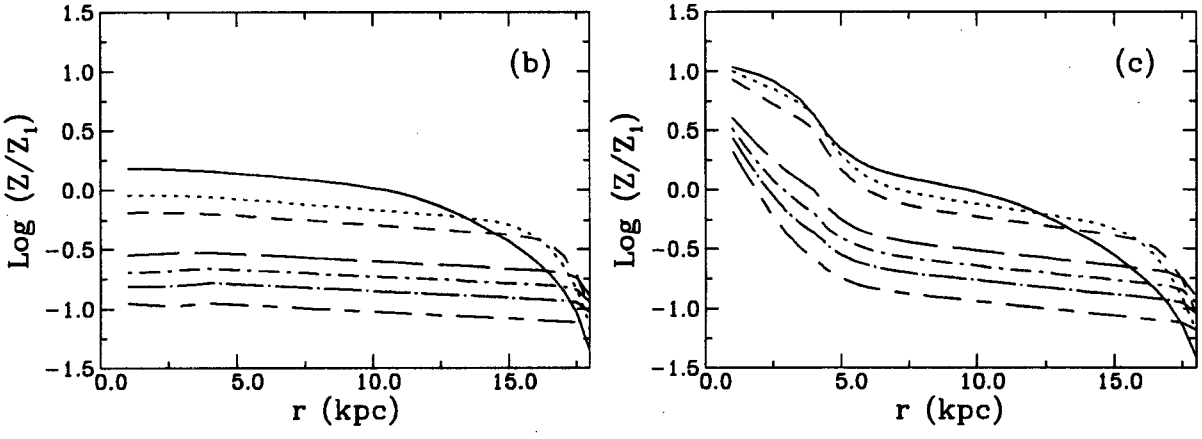

Fig. 3.(b,c) The temporal variation of metallicity gradient in the disk for model Y_1 (b) and Y_2 (c). Line legends are the same as in Fig. 1.

assumption of the SN I explosion rate as an exponential function with scale radius of 0.8 kpc in order to fit the observed abundance gradient in the solar neighborhood. This model fits the observed abundance distribution quite better than model Y_1. In Fig. 3b and Fig. 3c, the abundance gradient change with evolution time shows that the

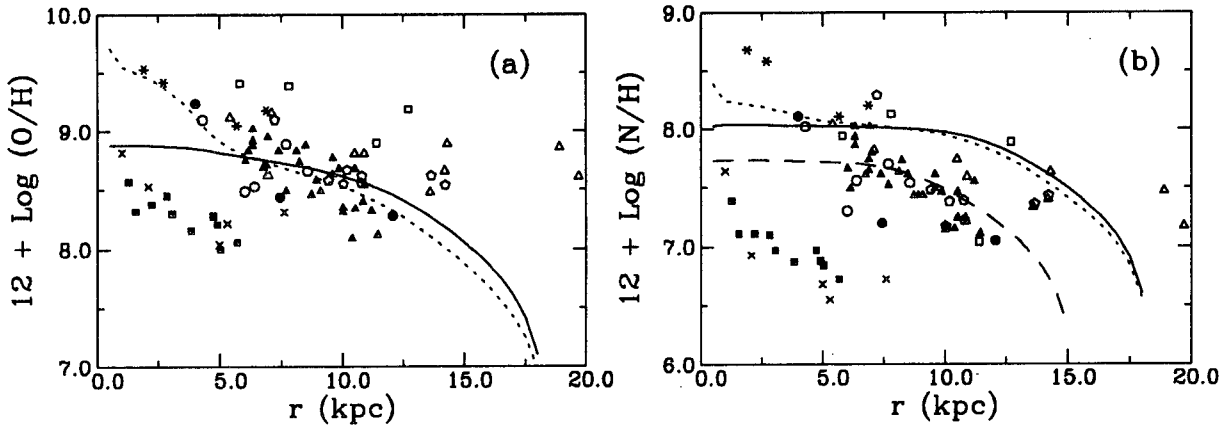

Fig. 4. The radial distribution of oxygen (a) and nitrogen (b) abundances in the disk. Observed data are denoted as follows; filled triangle : MWG, open triangle : M31, filled square : M 33, open square : M 51, snow mark : M 83, open pentagon : M 101, cross : NGC 2403, open circle : NGC 6946, and filled circle : IC 342 (Díaz & Tosi 1986). Solid line represents model Y_1 and dotted line represents model Y_2. Long dashed line in Fig. (b) represents model Z_1 in which the SFR cutoff radius is 15kpc.

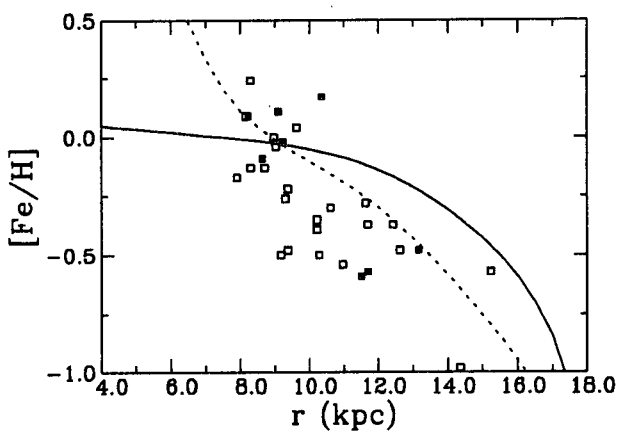

Fig. 5. The radial profile of [Fe/H] in the disk. Solid and dotted lines represent model Y_1 and Y_2, respectively. Open squares are observed data given by Friel & Janes(1993), and filled squares by Lynga(1987).

gradient is getting steeper and going inward as the evolution proceeds. This result is supported by the observational study of stars having the age difference of $\sim$ 2Gyrs in which younger stars show a steeper abundance gradient than older stars (Mayor 1976, Panagia and Tosi 1981).

For a comparison with the observed abundance distribution of external galaxies, observed oxygen and nitrogen abundances of some external spiral galaxies as well as our Galaxy (MWG) are plotted in Fig. 4 in which our computed results are compared. The data in figures are compiled from Díaz and Tosi (1986) and Shaver *et al.* (1983). The central radius of each external galaxy in Fig. 4 is transformed by multiplying the effective radius of our Galaxy with the normalized radius of each external galaxy using effective radius. Observed oxygen abundance gradient increases with relatively large dispersion toward the galactic center in Fig. 4a. In model Y_1, calculated abundance gradient does not match the observation near the galactic center, but in model Y_2 which assumed an exponential increase of SN I explosion rate toward the galactic center, it fits well the observation.

Nitrogen is produced by relatively low mass stars compared to oxygen which is produced from massive stars ($m \geq 10m_{\odot}$), and it is rarely produced by SN I. But it shows relatively a steep abundance gradient along the whole galactic disk and this is not fitted by both model Y_1 and Y_2. The large discrepancy between the observed nitrogen abundance gradient and computed ones can be explained as follows.

Most nitrogen is produced from intermediate mass stars as primary or secondary element. The evolution of these

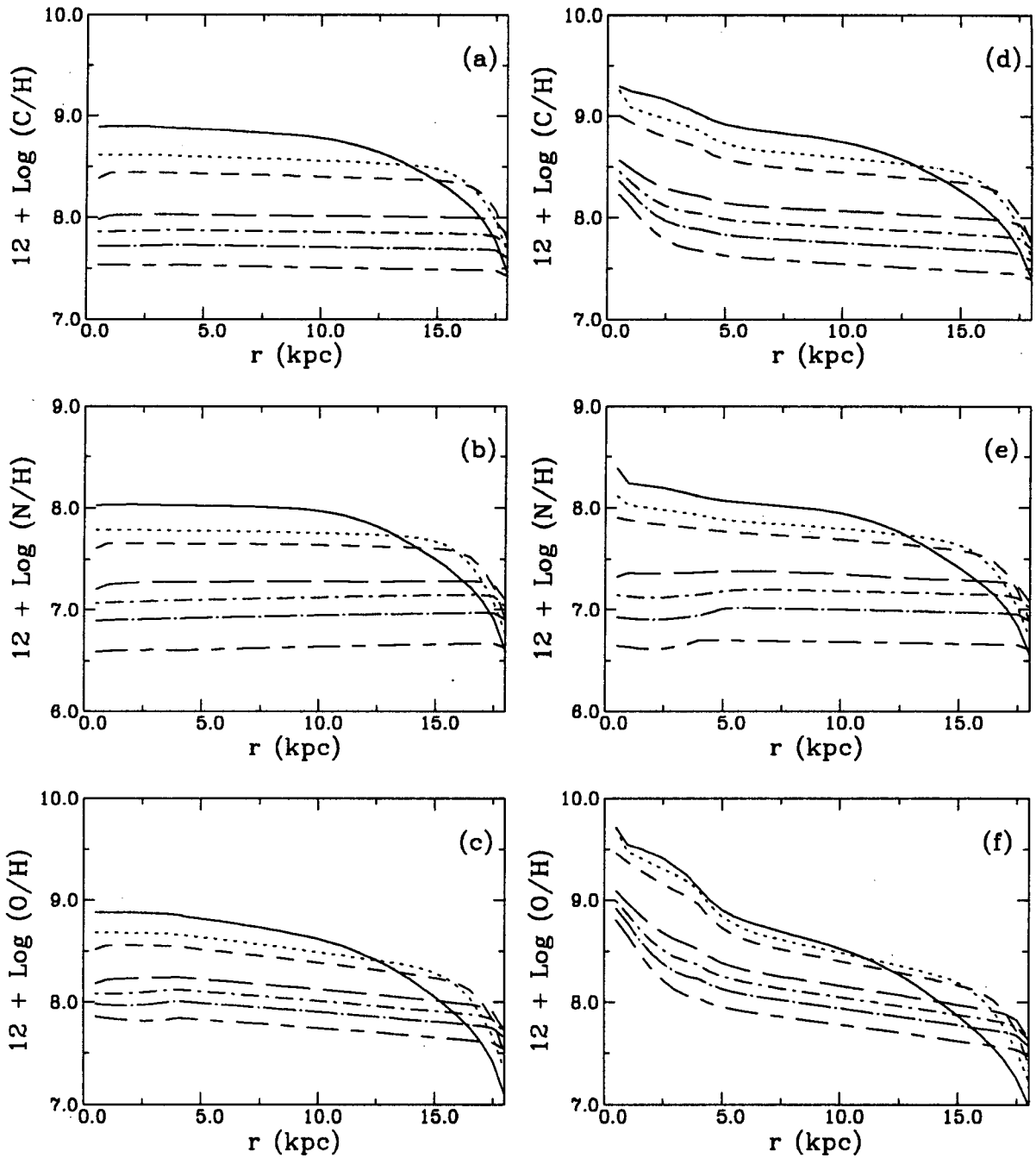

Fig. 6. Temporal variation of C, N, O distribution in the disk. Figures (a) – (c) are for model Y_1 and (d) – (f) are for model Y_2. Line legends are the same as in Fig. 1.

stars is affected by mass ejection and mixing length in convective outer shell during their lifetime. In other words, the intermediate mass star experiences three phases of dredge-up phenomena occurred in the hydrogen shell burning phase in red giant branch (RGB), in the helium shell burning phase, and in the shell flash phase of asymptotic giant branch (AGB). These dredge-up pulls out the elements, especially nitrogen inside the star to the surface of the star. The primary nitrogen is produced by the shell flashes at the AGB phase and the secondary nitrogen is produced by the CNO cycle in the dredge-up at the RGB and HB phases. Thus the nitrogen synthesis during the stellar evolution depends not only on the initial mass but also on the assumption of these variables (Renzini and Voli 1981, Díaz 1989). Moreover, primary nitrogen is produced by the hot-bottom burning process in the convective

outer shell during the AGB phase. The upper limit of these stars' mass is affected by convective overshooting and semiconvection which have not been proved in detail yet. So the nucleosynthesis prescription of nitrogen element varies widely with the variation of adopted variables and stellar evolution models. To fit the observed nitrogen abundance gradient more precisely, it is necessary to discuss carefully on the nucleosynthesis prescription for the nitrogen used in this model. In Fig. 4b, model Z_1 has the SFR cutoff radius at 15 kpc rather than 18 kpc, which is an example which tries to fit the observed nitrogen abundance gradient without changing nitrogen synthesis model.

Considering a relatively good fitness of the distribution of the other physical properties with observations, the nitrogen problem in this model is not thought to come from the IMF but the adopted nitrogen synthesis model seems to be problematic, i.e., for low mass stars, the primary nitrogen in the AGB phase or secondary nitrogen in the RGB or HB phase might be overestimated.

The observed iron abundance distribution of red giants in 24 open clusters of age more than 1 Gyr in the range of 7.9 $\sim$ 15.4 kpc is shown in Fig. 5. The results of our models are close to the upper boundary of the observed distribution at the outer region than the solar radius and close to the observed distribution at the inner region than the solar radius in Fig. 5. The steeper gradient of iron abundance in the inner region of the disk in model Y_2 shows a significant role of SN I in iron enrichment.

VI. CONCLUDING REMARKS

In the halo-disk model of the chemical evolution of our Galaxy, the disk evolution is highly subject to the infalling matter from the halo. In this model, the disk starts its evolution 0.08 Gyr after the initial galaxy formation. At that time the disk mass is about 30% of the present mass (Lee *et al.* 1991).

By adopting the central spike model as the radial velocity field model (Lacey and Fall 1985), our model can explain the observed gas and stellar density distribution which decrease from $r = 4$ kpc inward to the galactic center and then increase again. In the outer region of the Galaxy $r > 18$ kpc, where stars are no longer born, high density gas matter flows inward and as a result, the density gradient becomes flatter as radius increases.

The resulting exponents of the power law SFR which best explain the observational constraints are $n_2 = 1.0$ in Y_1 model and $n_2 = 1.1$ in Y_2 model, respectively. Though this model can explain observed density gradient in the Galaxy, the assumtion of the infall rate from the halo which is proportional to the SFR is not sufficient to reproduce the observed abundance gradient. For the abundance gradient, the radial gas flow in the disk and star formation boundary in the outer region of the disk are required.

The abundance gradient calculated in our models is nearly flat inside the solar radius and getting steeper outside, and as the disk evolution proceeds, the gradient expands inward and is being steeper. The abundance gradients obtained in model Y_1 fit well the observed abundance gradient outer than the solar radius, but it is flatter than the observation inside. But if we adopt the observed result in which the abundance gradient is nearly invariant along the whole disk (Shaver *et al.* 1983), we propose model Y_2 in which we additionally assume the exponential increase of SN I explosion rate inward the disk center. In Fig. 6, We also show the temporal evolution of oxygen, carbon and nitrogen abundance along the disk by using the models Y_1 and Y_2. It is noted that the computed distribution obtained by model Y_2 cover well the observed distributions of O/H and N/H in external galaxies as shown in Fig. 4. The results of the model Y_2 explain the observed abundance gradients in the disk relatively better than those of the model Y_1, which implies the significance of SN I in disk evolution.

ACKNOWLEDGEMENT

One of the author (B.-G. Park) appreciates very much to Mr. S.-L. Kim for his kind reading and suggestion for preparing figures and tables in this paper.

REFERENCES

Belley, J. & Roy, J.-R. 1992, ApJS 78, 61

Bhat, C. L., Houston, B. P., Issa, M. R., Mayer, C. J. & Wolfendale, A. W. 1984, in Gas in the Interstellar Medium,

ed. P. M. Gondalekhar
————. 1985, Nature 314, 511
Bond, H. E. 1970, ApJS 22, 117
Burton, W. B., & Gordon, M. A. 1978, A&A 63, 7
Carbon, D. F., Barbuy, B., Kraft, R. P., Friel, E. & Suntzeff, N. B. 1987, PASP 99, 335
Carlberg, R. G., Dawson, P. C. Hsu, T. & VandenBerg, D. A. 1985, ApJ 294, 674
Chromey, F. R. 1978, AJ 83, 162
Cohen, R. S., Thaddeus, P. & Bronfman, L. 1984, in IAU Symposium 106, The Milky Way Galaxy, eds H. van Wœrden, W. B. Burton & K. J. Allen (Dordrecht: Reidel)
Conte, S. D. & de Boor, Carl 1980, in Elementary Numerical Analysis - An Algorithmic Approach, 3rd ed., pp. 319-328 (McGraw-Hill, Inc.)
Díaz, A. I., & Tosi, M. 1986, A&A 158, 60
Díaz, A. I. 1989, in Evolutionary Phenomena in Galaxies, eds H. A. Thronson, Jr., & J. M. Shull (Dordrecht: Kluwer), p. 257
Dufour, R. J., Talbot, R. J., Jensen, E. P. & Shields, G. 1980, ApJ 236, 119
Fich, M. & Blitz, L. 1984, ApJ 279, 125
Fitzsimmons, A., Brown, P. J. F., Dufton, P. L. & Lennon, D. J. 1990, A&Ap 232, 437
Garnett, D. R. & Shield, G. A. 1987, ApJ 317, 82
Gehren, T., Nissen, P. E., Kudritzki, R. P. & Butler, K. 1985, in Production and Distribution of the CNO Elements, eds. I. J. Danziger, F. Matteucci, & K. Kjär (ESO pub.), p. 171
Gilmore, G. & Wyse, R. F. G. 1985, AJ 90, 2015
Goldreich, P. & Lynden-Bell, D. 1965, MNRAS 130,125
Gordon, M. A. & Burton, W. B. 1976, ApJ 208, 346
Hartkopf, W. I. & Yoss, K. M. 1982, AJ 87, 1679
Henderson, A. P., Jackson, P. D. & Kerr, F. J. 1982, ApJ 263, 116
Janes, K. A. 1979, ApJS 39, 154
Kang, Y. H. 1993, Ph. D. Thesis, Seoul National Univ.
Kennicutt, R. C. 1983, ApJ 272, 54
————. 1989, ApJ 344, 685
Kulkarni, S. R., Blitz, L. & Heiles, C. 1982, ApJL 259, L63
Lacey, C. G. & Fall, S. M. 1985, ApJ 290, 154
Laird, J. 1985, ApJ 289, 556
Lee, S.-W. & Ann, H. B. 1981, JKAS 14, 55
Lee, S.-W., Ann, H. B. & Sung, W. 1989, JKAS 22, 43
Lee, S.-W. & Chun, M.-Y. 1986, JKAS 19, 51
Lee, S.-W., Park, B.-G., Kang, Y. H. & Ann, H. B. 1991, JKAS 24, 25 (paper I)
Maciel, W. 1991, in Elements and The Cosmos, eds. M. G. Edmunds, B. E. J. Pagel & R. J. Terlevich (Cambridge Univ. Press)
Matteucci, F. & François, P. 1989, MNRAS 239, 885
Mayor, M. 1976, A&A 48, 301
Miller, G. E. & Scalo, J. M. 1979, ApJS 41, 513
Neese, C. L. & Yoss, K. M. 1988, AJ 95, 463
Nissen, P. E., Edvardsson, B. & Gustaffsson, B. 1985, in Production and Distribution of CNO Elements, eds. I. J. Danziger, F. Matteucci, & K. Kjär (ESO pub.), p. 131
Pagel, B. E. J. 1981, in The Structure and Evolution of Normal Galaxies, eds. S. M. Fall & D. Lynden-Bell (Cambridge Univ. Press), p. 211
————. 1985, in Production and Distribution of CNO Elements, eds. I. J. Danziger, F. Matteucci, & K. Kjär (ESO pub.), p. 155
————. 1987, in The Galaxy, eds. G. Gilmore & B. Carswell (D. Reidel pub. Co.), p. 341
Pagel, B. E. J. & Edmunds, M. G. 1981, ARAA 19, 77

Panagia, N. & Tosi, M. 1981, in High Energy Phenomena Around Collapsed Stars, ed. F. Pacini (Dordrecht: Reidel), p.33
Park, B.-G. 1991, M. S. Thesis, Seoul National Univ.
Renzini, A. & Voli, M. 1981, A&A 94, 175
Sancisi, R. 1983, in IAU Symposium 100, Internal Kinematics and Dynamics of Galaxies, ed. E. Athanassoula (Dordrecht: Reidel), p.55
Scalo, J. M. 1986, Fund. Cosmic Phys. 11, 1
Schmidt, M. 1959, ApJ 129, 243
————. 1963, ApJ 137, 758
Shaver, P. A., McGee, R. X., Danks, A. C. & Pottasch, S. R. 1983, MNRAS 204, 53
Tinsley, B. M. 1980, Fund. Cosmic Phys. 5, 287
Tomkin, J. & Lambert, D. L. 1984, ApJ 279, 220
Tomkin, J., Sneden, C. & Lambert, D. L. 1986, ApJ 302, 415
Tosi, M. 1982, ApJ 254, 699
Twarog, B. A. 1980, ApJ 242, 242
van den Bergh, S. 1962, ApJ 67, 486
van der Kruit, P. C. & Searle, L. 1982, A&A 110, 61
Wielen, R. 1977, A&A 60, 263